

Performance Improvement of Rotor Flux and Electromagnetic Torque Control in Induction Motors using the Backstepping Super-Twisting Algorithm

Dalal Zellouma
LEVRES Laboratory, Dep. of
Electrical Engineering,
University of El Oued
El Oued, Algeria
zellouma-dalal@univ-eloued.dz

Youcef Bekakra
LEVRES Laboratory, Faculty
of Technology, University of
El Oued, 39000 El Oued,
Algeria.
youcef-bekakra@univ-eloued.dz

Habib Benbouhenni
Faculty of Engineering and
Architecture, Department of
Electrical & Electronics
Engineering, Nisantasi
University,
Istanbul, Turkey;
habib.benbouhenni@nisantasi.edu.tr

Abstract – This paper presents the amelioration of rotor flux and electromagnetic torque ripples of the Inductions motors using backstepping control based on super twisting algorithms and pulse width modulation to control the motor inverter. The primary role of the backstepping management based on super-twisting algorithms is to control and regulate the torque and flux of induction motor drives. The field-oriented control is a traditional control scheme based on a proportional-integral controller, where durability is the biggest problem with this strategy. Backstepping control based on super twisting algorithms is a new control scheme; characterized by robustness, which gives a good response dynamic, minimum torque/flux ripples, and reduces harmonic distortion of current compared to other techniques such as direct torque control. The proposed control scheme construction is based on backstepping control and super twisting algorithm to obtain a robust control and minimize the induction motor's steady-state performance and overshoot of torque and flux. We use our study as a 1.5 KW induction motor to reduce the torque, current, and flux ripples. As shown in the resulting figures, the backstepping control based on the super twisting algorithm ameliorates effectiveness and especially minimizes the flux, torque, and current ripples. It also reduces harmonic distortion of current compared to classical technique.

Keywords- *induction motor; backstepping control; Lyapunov; sliding mode control; super-twisting algorithm; total harmonic distortion*

I. INTRODUCTION

Due to their high performance, and robustness, induction motors (IMs) are crucial in modern industry [1], [2]. The nonlinear component of fluxes and currents is used in IMs to determine torque. Because of their non-linear configuration, induction motors require complex control algorithms [3], [4], [5]. However, since the nonlinear characteristics and parameters vary with operating conditions, the control of IM is very complicated [6]. 1970, F. Blaschke published the first paper on field-oriented control (FOC) of induction motors [7], [8], [9]. In FOC techniques, traditional

proportional-integral (PI) controllers are Significant [10]. Regardless, PI controllers cannot achieve high dynamic performance [11], [12].

Numerous nonlinear control strategies for controlling the induction motor were studied [13].

To regulate the induction motor, new non-linear technologies are used, such as the FOC technique [14], direct torque control (DTC), predictive torque control (PTC) [15], backstepping control (BC) [16], sliding mode control (SMC) [17] and super twisting sliding mode (STSM) control algorithm [18], [19].

The Backstepping regulation has been a major success in the control of non-linear dynamic systems in different domains since its invention in its current form by Krstic Kanella kopoulos and Kokotovic [20]. The creation of stabilizing principle is based on the Lyapunov theory function.

Sliding Mode Control (SMC) initially emerged in 1930, and Itkis and Utkin pioneered the development of sliding mode theory and applications in the 1970s [21]. Several writers are now researching the applicability of this approach to the induction machine.

We may now utilize the SMC technique instead of classic control schemes thanks to the advancement of variable structure systems (VSS) theories.

SMC technique is an approach to controlling an induction motor that delivers it with high dynamic characteristics. In addition, it demonstrates great robustness and minimal software and hardware implementation. The primary drawback of this technique, though, is the chattering phenomenon [22]. The following are the primary benefits of using the SMC technique: control that is robust and insensitive to parameter changes.

A Lyapunov function principle is used to verify the stability of backstepping control, SMC-backstepping, and STSM-backstepping controllers.

Matlab/Simulink will be used to test and evaluate the performance and comparison between the proposed techniques. For the whole control system, the STSM-backstepping maintains rapid response with high robustness against dynamic conditions; it has the advantages to be robust to machine dynamical different versions and showing good reference tracking.

A numerical simulation of the developed control approach will be shown and examined in comparison with traditional control techniques. The efficiency of the suggested control mechanism and minimize total harmonic distortion (THD) is also detected harmonic distortion of stator current.

These are the main benefits of this study:

- Robustness to parameter variations;
- Reduce error tracking rotor speed and rotor flux references with STSM-Backstepping control scheme of induction motor;
- Response time is shorter and the chattering phenomenon is minimized;
- Minimizes the THD of stator currents and torque ripple.

The rest of the work is organized as follows: the modeling of the Induction Motor in Park's coordinates system (d-q) is displayed in Section 2. The traditional backstepping control structure with Lyapunov function is presented in section 3. Section 4 gives an overview of sliding mode controller of induction motor by Backstepping control. In Section 5, the super twisting sliding mode (STSM) algorithm is based on the backstepping controller. Results from simulations using MATLAB SIMULINK of the performances of various controllers are shown in Section 6.

II. Modeling of Induction Motor

The FOC principle of the field vector control induction machine is used to formulate a basic model of the induction machine that is similar to the direct current machine. A park transformation matrix is used in the induction motor strategy.

The equivalent three-phase fixed frame reference variables model of IM is modified to a two-phase fixed frame reference variables model. The following equation (1-4) is used as a representation of the model:

$$\frac{di_{sd}}{dt} = N_1 i_{sd} + \omega_s i_{sq} + N_2 \varphi_{rd} + \delta V_{sd} \quad (1)$$

$$\frac{di_{sq}}{dt} = N_1 i_{sq} - \omega_s i_{sd} - N_3 \omega \varphi_{rd} + \delta V_{sq} \quad (2)$$

$$\frac{d\varphi_{rd}}{dt} = \frac{M}{T_r} i_{sd} - \frac{1}{T_r} \varphi_{rd} \quad (3)$$

$$\frac{d\Omega}{dt} = \frac{3}{2} \frac{pM}{JL_r} \varphi_{rd} i_{sq} - \frac{T_L}{J} - \frac{f}{J} \Omega \quad (4)$$

Where:

$V_{sd} V_{sq}$: are defined as the rotor of dq-axis voltage
 R_s and R_r :The stator and rotor resistances.

φ_{rd} : are demonstrated as the d- axis rotor of flux.

ω_s and ω : electrical speed and reference speed rotation.

Ω : is stated as the mechanical rotor speed (rad/s),
 T_L : is stated as the mechanical torque (N.m),
The induction motor is defined by two equations (5) at the system d-q orientated axes:

$$\begin{aligned} \dot{x} &= A[x] + B[u] \\ y &= C[x] \end{aligned} \quad (5)$$

Where:

$$\begin{aligned} \dot{x} &= [i_{sd} \ i_{sq} \ \varphi_{rd} \ \varphi_{rq}]^t ; u = [V_{sd} \ V_{sq}]^t ; \\ y &= [i_{sd} \ i_{sq}] \end{aligned}$$

x is the state vector, u is the input vector, and y is the output vector.

$$A = \begin{bmatrix} N_1 & 0 & N_2 & N_3 \\ 0 & N_1 & -N_3 & N_2 \\ \frac{M}{T_r} & 0 & -\frac{1}{T_r} & 0 \\ 0 & \frac{M}{T_r} & 0 & -\frac{1}{T_r} \end{bmatrix} ; B = \begin{bmatrix} \delta & 0 \\ 0 & \delta \\ 0 & 0 \\ 0 & 0 \end{bmatrix} \quad (6)$$

$$C = \begin{bmatrix} 1 & 0 & 0 & 0 \\ 0 & 1 & 0 & 0 \end{bmatrix}$$

$$[P] = \sqrt{\frac{2}{3}} \begin{bmatrix} \cos \theta & \cos(\theta - \frac{2\pi}{3}) & \cos(\theta - \frac{4\pi}{3}) \\ -\sin \theta & -\sin(\theta - \frac{2\pi}{3}) & -\sin(\theta - \frac{4\pi}{3}) \\ \frac{1}{\sqrt{2}} & \frac{1}{\sqrt{2}} & \frac{1}{\sqrt{2}} \end{bmatrix}$$

With:

$$N_1 = -\left(\frac{1}{\sigma T_s} + \frac{M^2}{\delta L_r T_r}\right), N_2 = \frac{M}{\delta L_r T_r} ; N_3 = \frac{M}{\delta L_r}, \delta = \frac{1}{\sigma L_s}, \sigma = \frac{M}{L_s L_r}, T_s = \frac{L_s}{R_s}, T_r = \frac{L_r}{R_r}$$

[P] Park Transformation Matrix.

III. CONTROL OF BACKSTEPPING

The backstepping approach is a recursive and systematic process for nonlinear control systems [23]. This will have a significant positive impact on the stability of the nonlinear system.

The stability of the nonlinear system will benefit greatly from this [24]. Choose a stable Lyapunov function that makes sure step-by-step stabilization on every formulation step, is a key component of the backstepping method for induction motors [25].

The design of the backstepping controller for induction motors involves two steps. Its first step in solving the problem is to select currents i_{sdref} and i_{sqref} according to speed Ω and rotor flux φ_{rd} to pursue their desirable control reference signal Ω_{ref} and φ_{ref} . The second step is dedicated to the structure of current loops:

Locate the V_{sd} and V_{sq} regulations for the currents i_{sd} and i_{sq} fast convergence to required references i_{sdref} and i_{sqref} , respectively [26] [27].

A. First Step

In backstepping control it starts with calculating speed error and flow error is written in equation (7) :

$$\begin{cases} e_1 = \Omega_{ref} - \Omega \\ e_3 = \varphi_{ref} - \varphi_{rd} \end{cases} \quad (7)$$

We get the results in equation (8) by deriving (3) and (4):

$$\begin{cases} \dot{e}_1 = \dot{\Omega}_{ref} - \dot{\Omega} \Rightarrow \dot{\Omega}_{ref} - \frac{3}{2} \frac{pM}{JL_r} \varphi_{rd} i_{sq} - \frac{T_L}{J} \\ \dot{e}_3 = \dot{\varphi}_{ref} - \dot{\varphi}_{rd} \Rightarrow \dot{\varphi}_{ref} - \frac{M}{T_r} i_{sd} + \frac{1}{T_r} \varphi_{rd} \end{cases} \quad (8)$$

e_1 and e_3 : are errors in speed, and rotor flux, respectively.

The first Lyapunov function V is chosen (9) as:

$$\begin{cases} V = \frac{1}{2} e_1^2 + \frac{1}{2} e_3^2 \Rightarrow V = e_1 \dot{e}_1 + e_3 \dot{e}_3 \\ \dot{V} = e_1 \left[\dot{\Omega}_{ref} - \frac{3}{2} \frac{pM}{JL_r} \varphi_{rd} i_{sq} - \frac{T_L}{J} \right] + e_3 \left[\dot{\varphi}_{ref} - \frac{M}{T_r} i_{sd} + \frac{1}{T_r} \varphi_{rd} \right] \end{cases} \quad (9)$$

Therefore, (10) can be rewritten as:

$$\dot{V} < 0 \Leftrightarrow -K_1 e_1^2 - K_3 e_3^2 \quad (10)$$

So, the control i_{sdref} and i_{sqref} stabilize asymptotically (11) as:

$$\begin{cases} i_{sqref} = \frac{2}{3} \frac{JL_r}{pM\varphi_{rd}} \left[\dot{\Omega}_{ref} + \frac{T_L}{J} + K_1 e_1 \right] \\ i_{sdref} = \frac{T_r}{M} \left[\dot{\varphi}_{ref} + \frac{1}{T_r} \varphi_{rd} + K_3 e_3 \right] \end{cases} \quad (11)$$

B. Second Step

The final step in the Backstepping control is to calculate the currents error using equation (12) :

$$\begin{cases} e_2 = i_{sqref} - i_{sq} \\ e_4 = i_{sdref} - i_{sd} \end{cases} \quad (12)$$

We obtain by deriving using (13):

$$\begin{cases} \dot{e}_2 = i_{sqref} - \dot{i}_{sq} \Rightarrow i_{sqref} + N_1 i_{sd} + \omega_s i_{sq} + N_3 \omega \varphi_{rd} - \delta V_{sq} \\ \dot{e}_4 = i_{sdref} - \dot{i}_{sd} \Rightarrow i_{sdref} + N_1 i_{sd} - \omega_s i_{sq} - N_2 \varphi_{rd} - \delta V_{sd} \end{cases} \quad (13)$$

The Lyapunov candidate V is chosen (14) as:

$$\begin{cases} V_e = \frac{1}{2} [e_1^2 + e_2^2 + e_3^2 + e_4^2] \Rightarrow \dot{V}_e = e_1 \dot{e}_1 + e_2 \dot{e}_2 + e_3 \dot{e}_3 + e_4 \dot{e}_4 \\ \dot{V}_e = \dot{V} + e_2 \dot{e}_2 + e_4 \dot{e}_4 \end{cases} \quad (14)$$

Therefore, (14) It can be rewritten as follows:

$$\dot{V}_e < 0 \Leftrightarrow \dot{e}_2 = -K_2 e_2; \quad \dot{e}_4 = -K_4 e_4$$

$$\begin{cases} V_{sq} = \delta \left[i_{sqref} + N_1 i_{sd} + \omega_s i_{sq} - N_3 \omega \varphi_{rd} + K_2 e_2 \right] \\ V_{sdref} = \delta \left[i_{sdref} + N_1 i_{sd} - \omega_s i_{sq} - N_2 \varphi_{rd} + K_4 e_4 \right] \end{cases} \quad (15)$$

The Backstepping control-based (PMW) controller for an induction machine IM, as shown in Fig.1. This technique is simple, efficient, robust, and has a short response time. In contrast, this new and improved control method reduced torque and flux ripples in comparison to the classical FOC strategy.

IV. DESCRIPTION OF THE SMC TECHNIQUE

Sliding mode control (SMC) is a nonlinear system control structure derived from variable structure control (VSC) that was created to overcome the problems of previous nonlinear control system designs [28], [29] [30]. This technique produces more stator current distortion harmonics, electromagnetic torque ripples.

The SMC method is divided into three phases, which are as follows:

- Selection of a switching surface
- The condition of convergence
- Calculation of control

A backstepping sliding mode controller has been developed to control the induction motor's speed tracking. The controller output is the stator voltage in the d-q reference frame [31].

A. Speed and flux regulation surface

The surface for speed and flux using equation (16):

$$\begin{cases} S(\Omega) = \Omega_{ref} - \Omega \\ S(\varphi_{rd}) = \varphi_{ref} - \varphi_{rd} \end{cases} \quad (16)$$

Induction motor have the following mechanical equation (17) :

$$\begin{cases} \dot{S}(\Omega) = \dot{\Omega}_{ref} - \frac{3}{2} \frac{pM}{JL_r} \varphi_{rd} i_{sq} - \frac{T_L}{J} \\ \dot{S}(\varphi_{rd}) = \dot{\varphi}_{ref} - \frac{M}{T_r} i_{sd} + \frac{1}{T_r} \varphi_{rd} \end{cases} \quad (17)$$

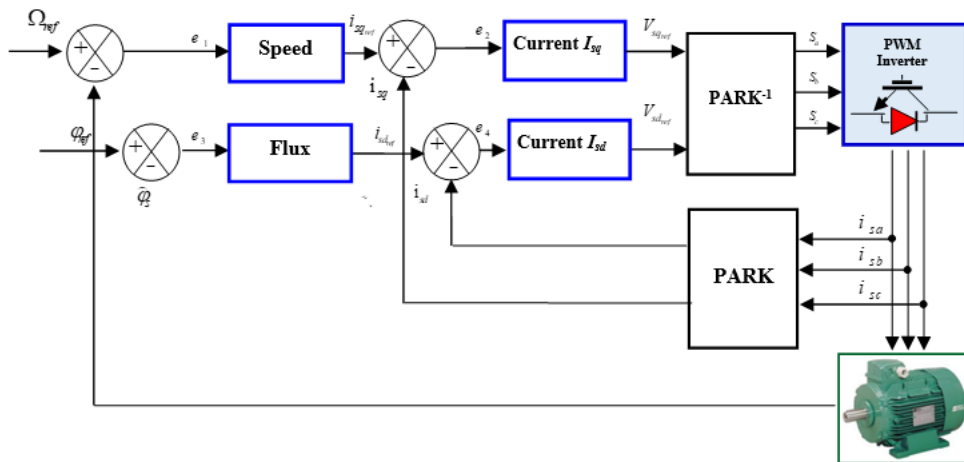


Figure 1. Block diagram of Backstepping control scheme for induction motor .

In sliding mode, take equation (18) :

$$\begin{cases} S(\Omega) = i_{sq}^{eq} + i_{sq}^n \\ S(\varphi_{rd}) = i_{sd}^{eq} + i_{sd}^n \end{cases} \quad (18)$$

Equation (19) represents the equivalent control :

$$\begin{cases} i_{sq}^{eq} = \frac{2}{3} \frac{JL_r}{pM\varphi_{rd}} \left(\dot{\Omega}_{ref} + \frac{T_L}{J} \right) \\ i_{sd}^{eq} = \frac{T_r}{M} \left(\dot{\varphi}_{ref} + \frac{1}{T_r} \varphi_{rd} \right) \end{cases} \quad (19)$$

And the switching control represents in Equation 20 :

$$\begin{cases} i_{sq}^n = K_{\Omega} \operatorname{sgn}(S(\Omega)) \\ i_{sd}^n = K_{\varphi_{rd}} \operatorname{sgn}(S(\varphi_{rd})) \end{cases} \quad (20)$$

B. Currents regulation surface i_{sq} and i_{sd} :

$$\begin{cases} S(i_{sq}) = i_{sq_{ref}} - i_{sq} \\ S(i_{sd}) = i_{sd_{ref}} - i_{sd} \end{cases} \quad (21)$$

Induction motor have the following mechanical equation in (22) :

$$\begin{cases} \dot{S}(i_{sq}) = i_{sq_{ref}} + N_1 i_{sd} + \omega_s i_{sq} + N_3 \omega \varphi_{rd} - \delta V_{sq} \\ \dot{S}(i_{sd}) = i_{sd_{ref}} + N_1 i_{sd} - \omega_s i_{sq} - N_2 \varphi_{rd} - \delta V_{sd} \end{cases} \quad (22)$$

In sliding mode, take equation (23) :

$$\begin{cases} S(i_{sq}) = V_{sq}^{eq} + V_{sq}^n \\ S(i_{sd}) = V_{sd}^{eq} + V_{sd}^n \end{cases} \quad (23)$$

with the equivalent control in equation (24) :

$$\begin{cases} V_{sq} = \delta (i_{sq_{ref}} + N_1 i_{sd} + \omega_s i_{sq} - N_3 \omega \varphi_{rd}) \\ V_{sd} = \delta (i_{sd_{ref}} + N_1 i_{sd} - \omega_s i_{sq} - N_2 \varphi_{rd}) \end{cases} \quad (24)$$

And the switching control in equation (25) :

$$\begin{cases} V_{sq}^n = K_{i_{sq}} \operatorname{sgn}(S(i_{sq})) \\ V_{sd}^n = K_{i_{sd}} \operatorname{sgn}(S(i_{sd})) \end{cases} \quad (25)$$

with:

$i_{sq}^{eq}; i_{sd}^{eq}; V_{sq}^{eq}; V_{sd}^{eq}$: Equivalent control,

$i_{sq}^n; i_{sd}^n; V_{sq}^n; V_{sd}^n$: switching control,

$K_{\Omega}; K_{\varphi_{rd}}; K_{i_{sq}}; K_{i_{sd}}$: is a positive gain.

V. DESCRIPTION OF THE STMS TECHNIQUE

For nonlinear system control, the super twisting algorithm STA sliding mode controller SMC has often been used.

This method is based on variable structure systems (VSS) theory [32], [33]. However, Utkin et al. introduced this technique in 1999 [34]. The STSM technique retains the characteristics of classic SMC methods. In comparison to other approaches, this algorithm, In addition, is straightforward to apply.

The STSM is used in this part to decrease flux and torque ripples while maintaining resilience and limited time convergence [35]. The control strategy is proposed by:

$$u = u_1 + u_2$$

The STSM algorithm's control method is stated as follows written in equation (26) :

$$\begin{cases} u_1(t) = K_1 \cdot \int \operatorname{Sgn}(S(t)) \cdot dt \\ u_2(t) = K_2 \cdot \sqrt{|S|} \cdot \operatorname{Sgn}(S(t)) \cdot dt \end{cases} \quad (26)$$

if $S(\infty) = 0$ we can simplify the technique.

K1 and K2 are positive gains utilized to adjust the STSM method, while S is the STSM algorithm switching function [36].

Fig. 2 shows a graphic representation of the STSM technique's control law. The basic configuration of the super-twisting sliding mode (STSM), algorithm of the induction motor is presented as shown in Fig. 3. This control technique was created to minimize chattering while also minimizing torque ripple and total harmonic distortion (THD).

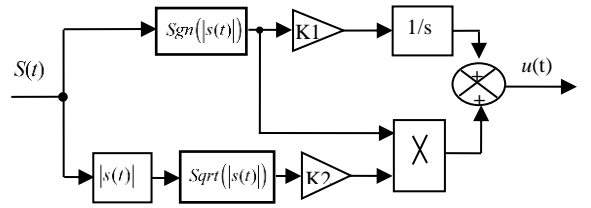


Figure 2. Block schematic of the STSM algorithm.

Compared to the traditional backstepping control, Sliding mode control (SMC). his technique is simple and robust,

with a short rise and response time.

VI. SIMULATION RESULTS

Numerical simulation in MATLAB/Simulink to verify the induction motor's functionality, stability, and robustness (IM). The parameters of a three-phase 1.5Kw induction motor are listed in the appendix.

To evaluate the performance of the three controllers: Backstepping, SMC-Backstepping, and STSM-Backstepping

- A nominal torque load (TL = 3.5 N.m) is applied at $t = 1.5$ sec.
- The simulation results for various speed profiles are shown in the following figures:
- A constant speed of 157 rad/sec
- A constant speed of 40 rad/sec

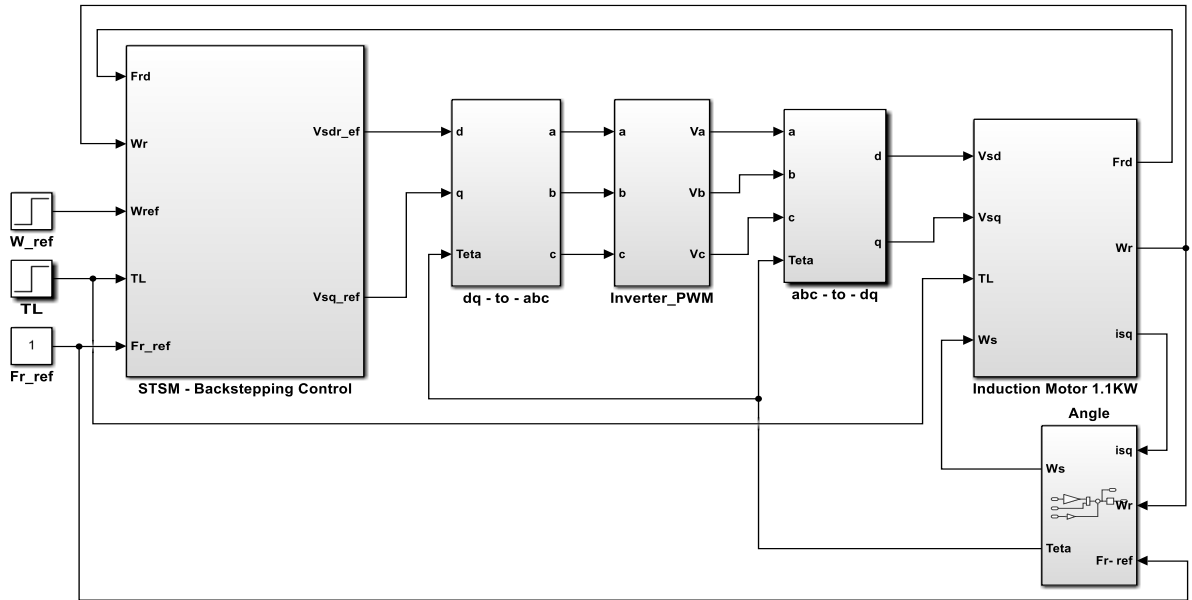
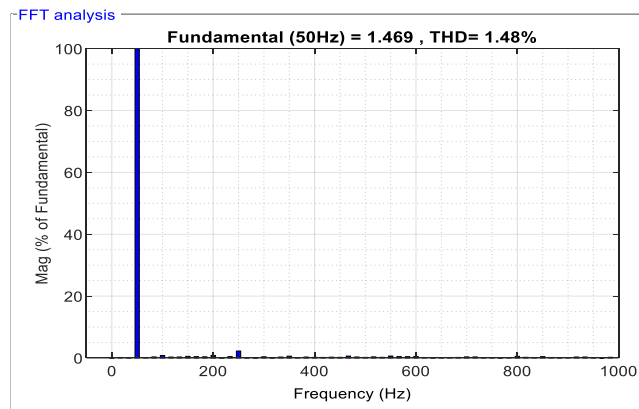


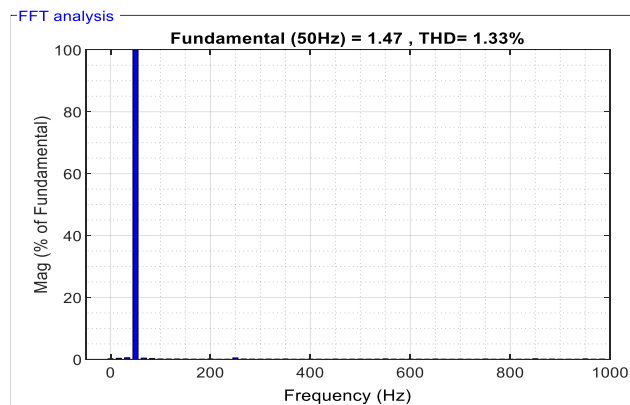
Figure 3. Simulink model of a 1.1W KM with STSM- Backstepping control

Fig. 4 shows the THD of stator phase current i_{sa} of an induction machine (IM). The Fast Fourier Transform (FFT) technique was used to generate the three controllers; when compared to Backstepping (THD =1.48%), SMC-Backstepping (THD =1.33%) and THD is clearly reduced with STSM-Backstepping supplied (THD =0.55%).

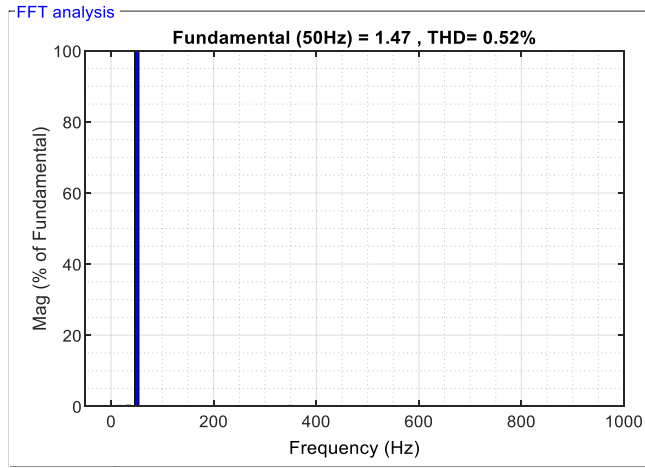
As a result, the proposed controller (STSM) effectively eliminates chattering and minimizes stator current harmonics.



a. THD of the Backstepping method.



b. THD of SMC-Backstepping method



c. THD of STMS-Backstepping method

Figure 4. THD for stator phase current isa.

A. Test the steady state

The simulation results are shown in Fig. 5 with a reference speed of 157 rad/sec and a load torque of 3.5 N.m applied at a time constant of 1.5 sec.

The intended reference value is followed by the rotation of the three controllers, with the STSM controller responding faster than the other two. After $t_r=0.4815$ sec for the STSM, $t_r=0.479$ sec for the SMC controller, and

$t_r=0.4573$ sec for the Backstepping controller, the speed approaches the reference 157rad/sec value.

The speed response of the backstepping and SMC controllers, on the other hand, has a short rise time, reaction time, and undershoot. Also, it has been noted that the STSM controller produces a torque that is less erratic when compared to conventional regulators, as seen in table 1.

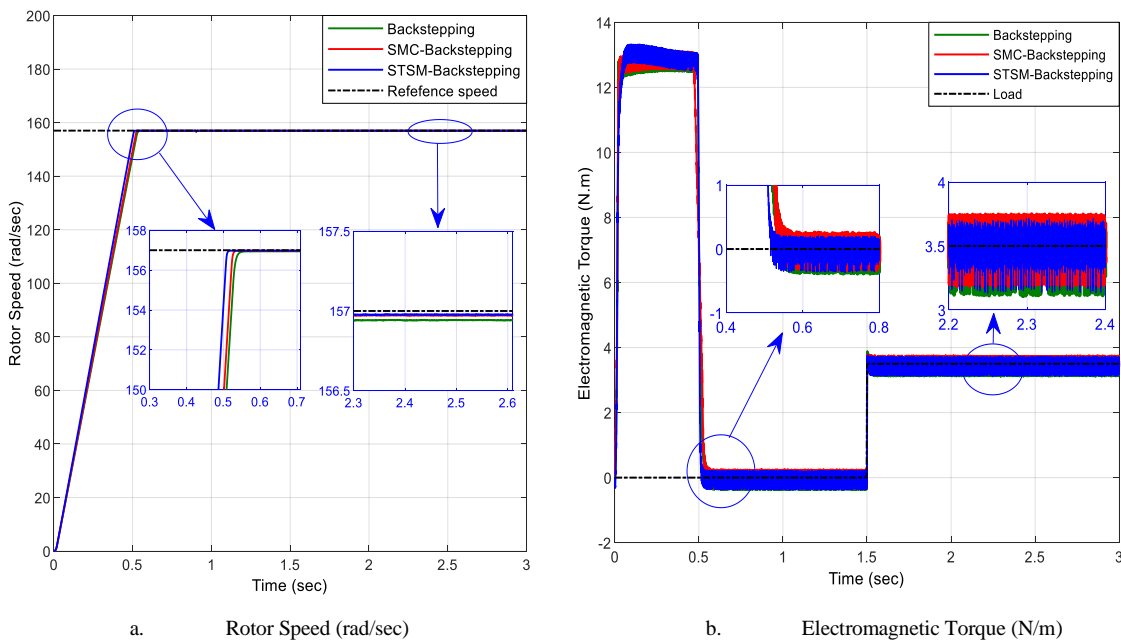


Figure 5. Steady-state: Speed response (157rad/sec) with load application at t=1.5 sec.

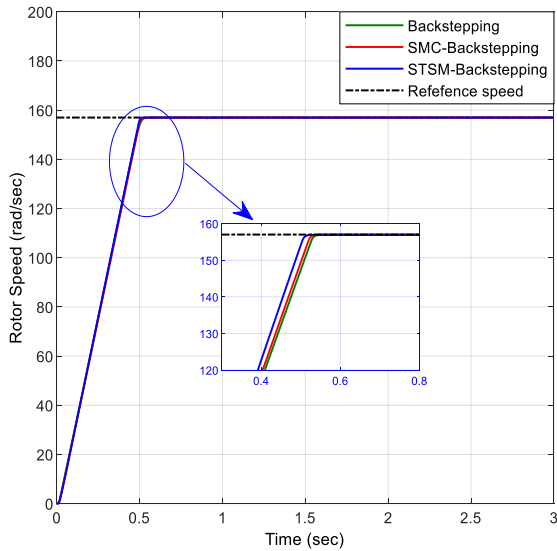
Table I COMPARATIVE PERFORMANCE OF THE THREE METHODS

Criteria		Methods	Backstepping	SMC-Backstepping	STSM-Backstepping
Response time (sec)	40rad/sec		0.14	0.1376	0.11
	157rad/sec		0.4815	0.479	0.4573
Rise time (sec)	40rad/sec		0.067	0.063	0.06
	157rad/sec		0.23	0.2	0.17
Static error ($\Omega_{ref} - \Omega$) (%)	40rad/sec		0.063	0.027	0
	157rad/sec		0.025	0.2	0
Torque ripples (%)	40rad/sec		16.42	15.42	10.14
	157rad/sec		16.42	15.88	8.5
Undershoot (Te %)	40rad/sec		0.07	0.025	0
	157rad/sec		0.063	0.025	0
THD (%)			1.48	1.33	0.52
Complexity			Simple	Simple	Simple
Robustness			Medium	Robust	Very Robust

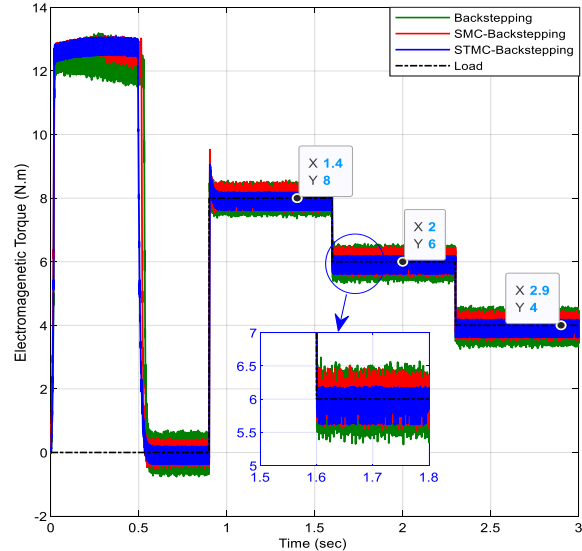
B. Variation in load torques

The second test in Fig. 6 depicts the system response behavior accomplished with Backstepping and SMC controllers, as well as Backstepping-STMS, following the application of variations in load torque, as shown in Fig. 6. with a torque load value of $T_L=[8 \ 6 \ 4]$ Nm and time $t=[1 \ 2 \ 3]$ sec.

When load torque is rapidly added and released, the STSM reacts faster than the Backstepping. The speed responses are unaffected by load torque changes and reject the load disturb exceptionally quickly with minimal overshoot and a negligible steady-state; torque ripple is also much reduced in STSM compared to the Backstepping controller.



a. Rotor Speed (rad/sec)



b. Electromagnetic Torque (N/m)

Figure 6. STMS, SMC, and Backstepping controller responses (under load torque variation)

C. Test Very low-speed

Fig. 7 shows how the Backstepping-STSM, Backstepping-SMC, and Backstepping controllers respond to speed in low-speed regions. A speed reference variation has been made in this test ($\Omega_{ref} = 40$ rad/sec). The Backstepping-STSM, in contrast to the Backstepping controller, maintained good dynamics even at low-speed values.

Torque changes under load and fast and without overshoot reject the load disturbance;

torque ripple is also minimized in STSM compared to the Backstepping controller

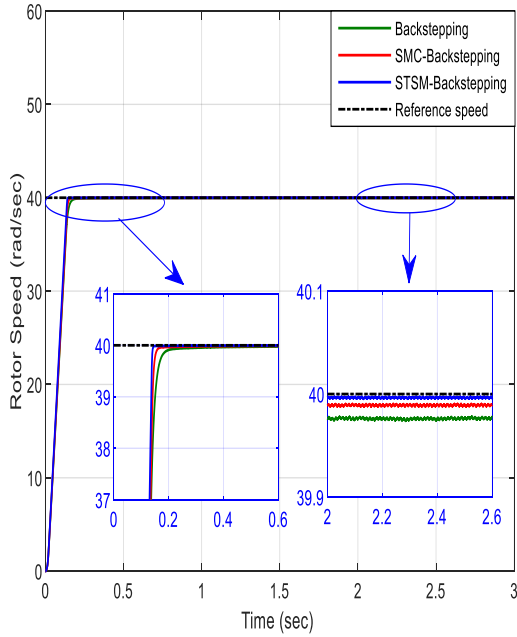
D. Test Very low-speed reference reversing

The simulation results for a trapezoidal speed set point with rotation reversal from 40 to -40 rad/sec. A steady torque of 3.5 N.m is given to the load starting at time $t = 1.5$ seconds. As seen in Fig. 8.

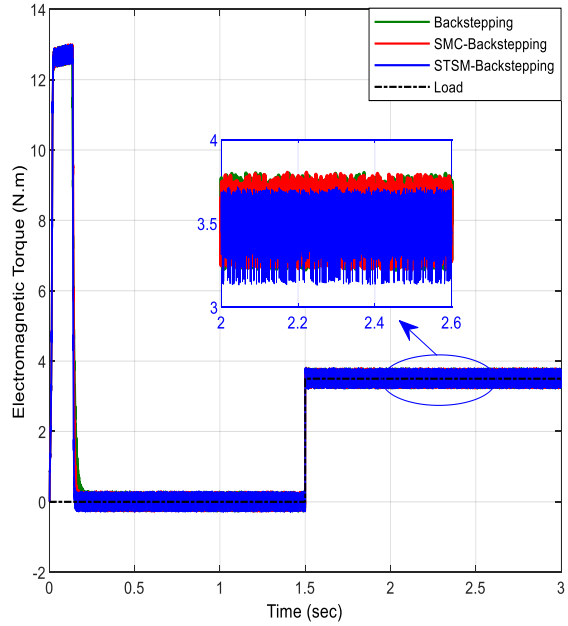
Compared to other controllers, the rotation speed of the STSM correctly and swiftly follows its reference value. The rotational direction can be reversed without undershooting.

The load torque is stabilized by electromagnetic torque because speed regulators rapidly speed or slow the speed in response to the reference torque.

A set point change and a change in rotational direction also cause the torque to the peak.

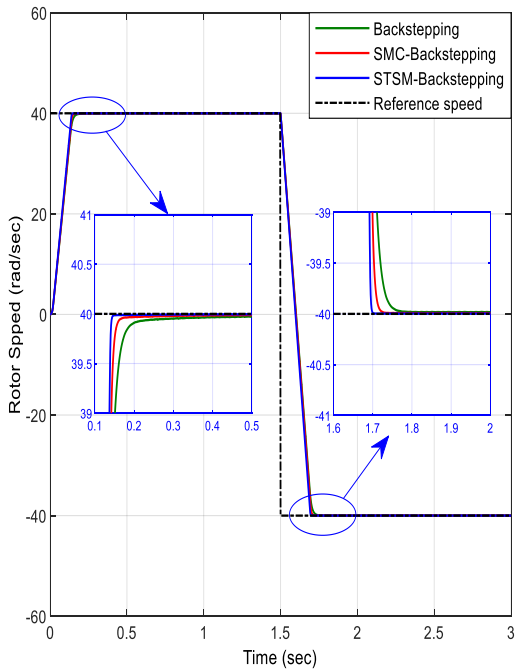


a. Rotor Speed (rad/sec)

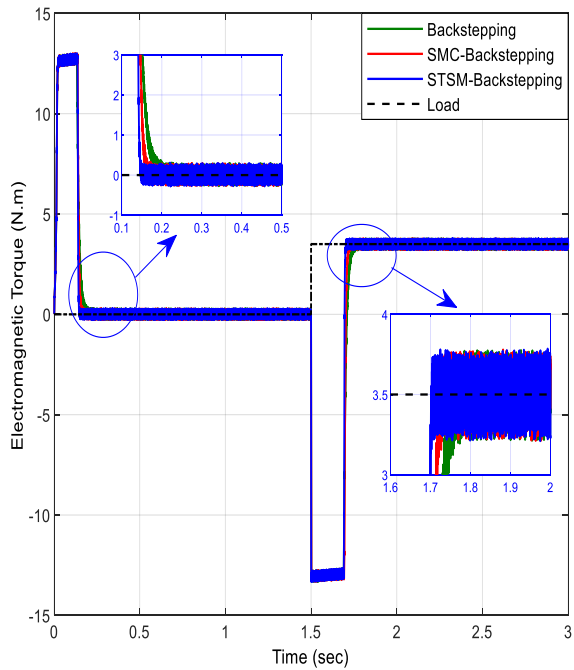


b. Electromagnetic Torque (N/m)

Figure 7. Test Very low-speed 40 rad/sec with load application at t=1.5 sec.



a. Rotor speed (rad/sec)



b. Electromagnetic Torque (N/m)

Figure 8. Test of speed reference reversing (40rad/sec -40 rad/sec).

The comparison of the THD value is shown in Table 2. As a result, the proposed STSM-based backstepping control is more robust than the STSM-based backstepping control system.

Table II TABLE COMPARISON OF THE OBTAINED RESULTS WITH OTHER METHODS

Reference	Technique	THD (%)
[37]	FOC	3.7
[38]	MRAS-SM-FOC	2.70
[39]	RSC Control Algorithm	12.17 to 12.09
[40]	ACHR	4.88% to 4.03%
[41]	DTC	12.23
	PTC	3.89
[42]	AST-PWM	6.86
	SST-PWM	6.69
[43]	SMC	2.06
	ASMC	1.91
	AFSMC	1.71
[44]	PTC	4.28
	FPTC	3.62
	MOFPTC	3.71
Proposed techniques	Backstepping	1.48
	SMC- Backstepping	1.33
	STSM- Backstepping	0.52

VII. CONCLUSION

This paper compares three control techniques for an induction motor, which are as follows: the traditional backstepping control technique, second the sliding mode control, and the third super twisting sliding mode controller technology, to limit torque and flux ripples, as well as stator current THD value. To increase the effectiveness and performance of the system control.

The stability of the Backstepping method was calculated using the Lyapunov stability concept.

Numerical simulation results obtained by Matlab/Simulink, Backstepping-STSM presents reasonable control, the simulation results indicate robustness and speed performance without static error. The stated controller under variable conditions, such as changing load torque and reference speed. The main findings are as follows:

- Reduce the chattering phenomenon;
- Reduce the torque and flux ripples;
- Minimized the Total harmonic distortion (THD);
- This designed control technique is small rise time and response time;
- Simple and robust technique.
- The coupling of Backstepping -Super twisting sliding mode controller with robust technique is a good solution for electrical machine control.

APPENDIX

TABLE III TABLE IMPLEMENTATION IM PARAMETERS

Parameters	Components	Values
Nominal power	p	1.5 KW
Load torque	T _L	3.5 N.m
Number of poles	p	2
Frequency	F	50 Hz
Stator resistance	R _s	5.35 Ω
Stator inductance	L _s	0.5763 H
Rotor resistance	R _r	4.05 Ω
Rotor inductance	L _r	0.5763 H
Mutual inductance	M	0.556 H
Inertia	J	0.0498 Kg.m ²
Friction	f	0 N.m.s

References

- [1] M. Sun, H. Wang, P. Liu, Z. Long, J. Yang, and S. Huang, "A Novel Data-Driven Mechanical Fault Diagnosis Method for Induction Motors Using Stator Current Signals," *IEEE Trans. Transp. Electrifi.*, vol. 7782, no. c, 2022, doi: 10.1109/TTE.2022.3163612.
- [2] H. R. Mohammadi and A. Akhavan, "Parameter Estimation of Three-Phase Induction Motor Using Hybrid of Genetic Algorithm and Particle Swarm Optimization," *J. Eng. (United Kingdom)*, vol. 2014, 2014, doi: 10.1155/2014/148204.
- [3] J. Yu, B. Chen, Y. Ma, and H. Yu, "Robust speed tracking control for the induction motor via adaptive fuzzy backstepping," *Proc. 2011 Chinese Control Decis. Conf. CCDC 2011*, pp. 2181–2184, 2011, doi: 10.1109/CCDC.2011.5968568.
- [4] N. El Ouanjli *et al.*, "Modern improvement techniques of direct torque control for induction motor drives-A review," *Prot. Control Mod. Power Syst.*, vol. 4, no. 1, 2019, doi: 10.1186/s41601-019-0125-5.
- [5] A. Véliz-tejo, J. C. Travieso-torres, A. A. Peters, A. Mora, and F. Leiva-silva, "Normalized-Model Reference System for Parameter Estimation of Induction Motors," pp. 1–29, 2022.
- [6] H. Xie, F. Wang, Q. Chen, Y. He, J. Rodriguez, and R. Kennel, "Computationally Efficient Predictive Current Control with Finite Set Extension using Derivative Projection for IM Drives," *IEEE J. Emerg. Sel. Top. Power Electron.*, vol. 6777, no. c, pp. 1–1, 2022, doi: 10.1109/jestpe.2022.3175904.
- [7] H. M. Soliman, "Performance characteristics of induction motor with field oriented control compared to direct torque control," *Int. J. Power Electron. Drive Syst.*, vol. 7, no. 4, pp. 1125–1133, 2016, doi: 10.11591/ijpeds.v7.i4.pp1125-1133.
- [8] A. T. Azar and Q. Zhu, *Advances and applications in sliding mode control systems*, vol. 576, no. January, 2015. doi: 10.1007/978-3-319-11173-5.
- [9] S. Vahid and H. Akbari, "Direct Field Oriented Control of Induction Motor (IM) Drive using Fuzzy Logic Controller (FLC)," no. Im.
- [10] S. Mahfoud, A. Derouich, N. El Ouanjli, T. Mohammed, and A. Hanafi, "Field oriented control of doubly fed induction motor using speed sliding mode controller," *E3S Web Conf.*, vol. 229, pp. 1–12, 2021, doi: 10.1051/e3sconf/202122901061.
- [11] M. J. Vallabhai, "PI Control Based Vector Control

- Strategy for Induction Motor Drive,” vol. 3, no. 2, pp. 328–335, 2012.
- [12] R. Gunabalan and V. Subbiah, “Speed Sensorless Vector Control of Induction Motor Drive with PI and Fuzzy Controller,” vol. 5, no. 3, p. 8694, 2015.
- [13] M. Fateh and R. Abdellatif, “Comparative study of integral and classical backstepping controllers in IFOC of induction motor fed by voltage source inverter,” *Int. J. Hydrogen Energy*, vol. 42, no. 28, pp. 17953–17964, 2017, doi: 10.1016/j.ijhydene.2017.04.292.
- [14] D. Zellouma, Y. Bekakra, and H. Benbouhenni, “Field-oriented control based on parallel proportional–integral controllers of induction motor drive,” *Energy Reports*, vol. 9, pp. 4846–4860, 2023, doi: 10.1016/j.egy.2023.04.008.
- [15] A. Ammar, B. Talbi, T. Ameid, Y. Azzoug, and A. Kerrache, “Predictive direct torque control with reduced ripples for induction motor drive based on T-S fuzzy speed controller,” *Asian J. Control*, vol. 21, no. 4, pp. 2155–2166, 2019, doi: 10.1002/asjc.2148.
- [16] T. Ameid *et al.*, “Hardware Implementation of Modified Backstepping Control for Sensorless Induction Motor Drive,” *IECON Proc. (Industrial Electron. Conf.)*, vol. 2019-October, pp. 1077–1082, 2019, doi: 10.1109/IECON.2019.8926795.
- [17] M. Drives, “An Enhanced Sliding Mode Speed Control for Induction Motor Drives,” pp. 1–14, 2022.
- [18] X. Xiong, S. Kamal, and S. Jin, “Adaptive gains to super-twisting technique for sliding mode design,” *Asian J. Control*, vol. 23, no. 1, pp. 362–373, 2021, doi: 10.1002/asjc.2202.
- [19] M. M. Ali, W. Xu, A. Junejo, M. Elmorshedy, and Y. Tang, “One new super-twisting sliding mode direct thrust control for linear induction machine based on linear metro,” *IEEE Trans. Power Electron.*, vol. 37, no. 1, pp. 795–805, Jan. 2022, doi: 10.1109/TPEL.2021.3096066.
- [20] Y. Zahraoui, M. Akherraz, and A. Ma’arif, “A Comparative Study of Nonlinear Control Schemes for Induction Motor Operation Improvement,” *Int. J. Robot. Control Syst.*, vol. 2, no. 1, pp. 1–17, 2021, doi: 10.31763/ijrcs.v2i1.521.
- [21] S. N. Makarov, “Antenna and EM Modeling with MATLAB -,” pp. 1–284, 2002.
- [22] B. Farid, B. Tarek, and B. Sebti, “Fuzzy super twisting algorithm dual direct torque control of doubly fed induction machine,” *Int. J. Electr. Comput. Eng.*, vol. 11, no. 5, pp. 3782–3790, Oct. 2021, doi: 10.11591/ijece.v11i5.pp3782-3790.
- [23] M. Taoussi, M. Karim, B. Bossoufi, D. Hammoumi, A. Lagrioui, and A. Derouich, “Speed variable adaptive backstepping control of the doubly-fed induction machine drive,” *Int. J. Autom. Control*, vol. 10, no. 1, pp. 12–33, 2016, doi: 10.1504/IJAAC.2016.075140.
- [24] B. Kelkoul and A. Boumediene, “Stability analysis and study between classical sliding mode control (SMC) and super twisting algorithm (STA) for doubly fed induction generator (DFIG) under wind turbine,” *Energy*, vol. 214, p. 118871, 2021, doi: 10.1016/j.energy.2020.118871.
- [25] M. M. Zirkohi, “An efficient approach for digital secure communication using adaptive backstepping fast terminal sliding mode control,” *Comput. Electr. Eng.*, vol. 76, pp. 311–322, 2019, doi: 10.1016/j.compeleceng.2019.04.007.
- [26] D. Zellouma, H. Benbouhenni, and Y. Bekakra, “Backstepping Control Based on a Third-order Sliding Mode Controller to Regulate the Torque and Flux of Asynchronous Motor Drive,” pp. 1–11, 2022.
- [27] R. Taleb, A. Bouchaib, and A. Namoune, “High Performance Backstepping Control of Induction Motor Fed by 19 Level Asymmetrical Inverter,” vol. 1, pp. 9–15, 2021.
- [28] K. D. Young, V. I. Utkin, and Ü. Özgüner, “A control engineer’s guide to sliding mode control,” *IEEE Trans. Control Syst. Technol.*, vol. 7, no. 3, pp. 328–342, 1999, doi: 10.1109/87.761053.
- [29] A. Nurettin and N. İnanç, “Hybrid Speed Controller Design Based on Sliding Mode Controller Performance Study for Vector Controlled Induction Motor Drives,” *Proc. Eng. Technol. Innov.*, vol. 19, pp. 01–15, 2021, doi: 10.46604/peti.2021.7717.
- [30] O. Boughazi, A. Boumediene, and H. Glaoui, “Sliding Mode Backstepping Control of Induction Motor,” *Int. J. Power Electron. Drive Syst.*, vol. 4, no. 4, pp. 481–488, 2014.
- [31] C. Chen and H. Yu, “Backstepping sliding mode control of induction motor based on disturbance observer,” *IET Electr. Power Appl.*, vol. 14, no. 12, pp. 2537–2546, 2020, doi: 10.1049/iet-epa.2020.0485.
- [32] B. Guo *et al.*, “A Robust Second-Order Sliding Mode Control for Single-Phase Photovoltaic Grid-Connected Voltage Source Inverter,” *IEEE Access*, vol. 7, pp. 53202–53212, 2019, doi: 10.1109/ACCESS.2019.2912033.
- [33] F. F. M. El-Sousy, M. M. Amin, and O. A. Mohammed, “Robust Adaptive Neural Network Tracking Control With Optimized Super-Twisting Sliding-Mode Technique for Induction Motor Drive System,” *IEEE Trans. Ind. Appl.*, vol. 58, no. 3, pp. 4134–4157, 2022, doi: 10.1109/TIA.2022.3160136.
- [34] V. I. Utkin, D. S. Chen, S. Zarei, and J. Miller, “Sliding mode observers for automotive alternators,” *Proc. Am. Control Conf.*, vol. 1, no. June, pp. 165–166, 1999, doi: 10.1109/acc.1999.782760.
- [35] F. Boumaraf, T. Boutabba, and S. Belkacem, “Dual direct torque control of doubly fed induction machine using second order sliding mode control,” *J. Meas. Eng.*, vol. 9, no. 1, pp. 1–12, 2021, doi: 10.21595/jme.2021.21432.
- [36] M. Horch, A. Boumediene, and L. Baghli, “Backstepping approach for nonlinear super twisting sliding mode control of an induction motor,” *3rd Int. Conf. Control. Eng. Inf. Technol. CEIT 2015*, 2015, doi: 10.1109/CEIT.2015.7233109.
- [37] F. Amrane, A. Chaiba, B. E. Babes, and S. Mekhilef, “Design and implementation of high performance field oriented control for grid-connected doubly fed induction generator via hysteresis rotor current controller,” *Rev. Roum. des Sci. Tech. Ser. Electrotech. Energ.*, vol. 61, no. 4, pp. 319–324, 2016.
- [38] S. Khadar, H. Abu-Rub, and A. Kouzou, “Sensorless Field-Oriented Control for Open-End Winding Five-Phase Induction Motor with Parameters Estimation,” *IEEE Open J. Ind. Electron. Soc.*, vol. 2, pp. 266–279, 2021, doi: 10.1109/OJIES.2021.3072232.
- [39] S. Puchalapalli and B. Singh, “A Novel Control Scheme for Wind Turbine Driven DFIG Interfaced to Utility Grid,” *IEEE Trans. Ind. Appl.*, vol. 56, no. 3, pp. 2925–2937, 2020, doi: 10.1109/TIA.2020.2969400.
- [40] A. Kazemtarghi, A. Chandwani, N. Ishraq, and A. Mallik, “Active Compensation-based Harmonic Reduction Technique to Mitigate Power Quality

- Impacts of EV Charging Systems,” 2022, doi: 10.1109/TTE.2022.3183478.
- [41] N. H. Viet and P. D. Dai, “A Comparison of DTC and PTC Techniques for Induction Motor Drive Systems,” *Proc. 13th Int. Conf. Electron. Comput. Artif. Intell. ECAI 2021*, 2021, doi: 10.1109/ECAI52376.2021.9515130.
- [42] S. K. Singh, “Synchronized Sine-triangle PWM Based Control of High-Speed PMSM Drive With Reduced Switching Losses and Enhanced Performance Department of Electrical Engineering,” 2022.
- [43] M. Benkahla, R. Taleb, and Z. Boudjema, “a New Robust Control Using Adaptive Fuzzy Sliding Mode Control for a Dfig Supplied By a 19-Level Inverter With Less Number of Switches,” *Electr. Eng. Electromechanics*, vol. 0, no. 4, pp. 11–19, 2018, doi: 10.20998/2074-272x.2018.4.02.
- [44] M. Mamdouh, A. Salem, and M. A. Abido, “An improved multi-objective fuzzy decision based predictive torque control of induction motor drive,” *Proc. IECON 2017 - 43rd Annu. Conf. IEEE Ind. Electron. Soc.*, vol. 2017-Janua, pp. 8675–8680, 2017, doi: 10.1109/IECON.2017.8217524.

